Strongly correlated systems in atomic and condensed matter physics

Lecture notes for Physics 284

by Eugene Demler

Harvard University

November 25, 2014

Chapter 16

Fermionic Hubbard model

16.1 Strongly correlated electron systems and the Hubbard model

Hubbard model is commonly used to describe strongly correlated electron systems especially in transition metals and transition metal oxides. These classes of materials include magnetic and non-magnetic Mott insulators, high temperature superconductors. Transition elements occupy three rows of the periodic table, extending from the alkali earths (Ca, Sr, Ba) to the noble metals (Cu, Ag, Au). The electronic d-shell is completely empty in the alkali earths and completely filled in the noble metals. Properties of all these materials are strongly dominated by the d-electrons. When electrons on the Fermi surface originate from the d orbitals, the tight-binding approximation provides a better model of the kinetic energy of electrons. Strongly localized character of d-orbitals implies that interactions between electrons on the same ion are much larger than interactions of electrons on different ions. This naturally leads to the effective model [2, 4, 28, 19]

$$\mathcal{H} = -t \sum_{\langle ij \rangle \sigma} c^{\dagger}_{i\sigma} c_{j\sigma} \; + \; U \sum_{i} n_{i\uparrow}\, n_{i\downarrow} \; - \mu \sum_{i} n_i \tag{16.1}$$

Here $n_{i\sigma} = c^{\dagger}_{i\sigma}\, c_{i\sigma}$ and $n_i = n_{i\uparrow} \, + \, n_{i\downarrow}$.

Soon after the discovery of high temperature superconductivity in cuprate materials P.W. Anderson pointed out the importance of repulsive interactions in these materials[3]. A simple Hubbard model correctly captures the insulating behavior of the parent compounds. Whether it captures high temperature superconductivity is still a subject of debate. During the last few decades analysis of the Hubbard model has been one of the mast active research areas in condensed matter physics. Hubbard model (and its extensions) is also used to describe organic materials[1].

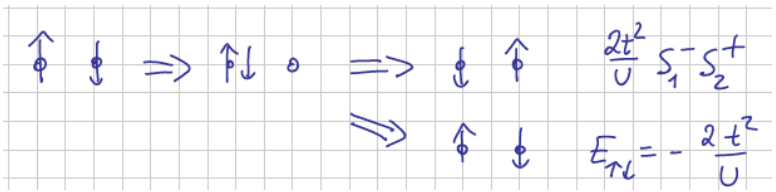

Figure 16.1: Derivation of the effective Heisenberg model from the Hubbard model. Electrons in a singlet configuration can regain some kinetic energy by doing virtual tunneling into doubly occupied configurations. Factors of 2 arise because tunneling processes can proceed in two ways (left to right and back or vice versa).

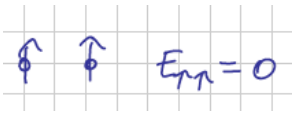

Figure 16.2: Derivation of the effective Heisenberg model from the Hubbard model. Electrons in a triplet configuration can not regain kinetic energy from virtual tunneling into doubly occupied configurations.

16.2 Antiferromagnetism in the Hubbard model

16.2.1 Strong coupling. Heisenberg model

We consider strong coupling limit of the Hubbard model ($U >> t$) at half-filling ($\langle n \rangle = 1$). When $t = 0$ all states that have exactly one fermion per site correspond to the degenerate manifold of the ground states. In order to lift this massive degeneracy we consider effects of fluctuations induced by the kinetic energy in the leading order in t/U. In an expansion in $\frac{t}{U}$ we integrate out virtual transitions into intermediate states in which one site becomes doubly occupied. This intermediate states have an energy U above that of the degenerate ground states. This procedure can be seen already in an example of two fermions in two sites in figs. 16.1, 16.2. A state with two spins in a singlet configuration can gain kinetic energy by tunneling virtually to states with double occuancies. We compare processes shown in figs. 16.1, 16.2. to an effective Heisenberg Hamiltonian

$$\mathcal{H} = J \vec{S}_1 \vec{S}_2 \tag{16.2}$$

and obtain

$$J = \frac{4t^2}{U} \tag{16.3}$$

By extending this analysis to an array of sites we obtain a Heisenberg model

$$\mathcal{H} = J \sum_{\langle ij \rangle} \vec{S}_i \vec{S}_j \tag{16.4}$$

In this chapter we will only consider fermionic Hubbard model on cubic lattices in d=2, 3, where the ground state has a character of the classical antiferromagnetic state. In d=1 exact theorems forbid the existence of the long range order. In this case the ground state can be obtained from the Bethe ansatz solution. In higher dimensions but on non bi-partite lattices, such as a triangular lattice, Hubbard models may exhibit exotic spin-liquid types of ground states even at filling factor one[18, 16].

16.2.2 Weak coupling

We can also study antiferromagnetic instability from the side of weak interactions. When $U = 0$

$$\mathcal{H} = \sum_{k\sigma} \epsilon_k c^\dagger_{k\sigma} c_{k\sigma}$$
$$\epsilon_k = -2t(\cos k_x + \cos k_y) - \mu \tag{16.5}$$

In the Hamiltonian (16.5) we took $d = 2$ and set lattice constant to one. At half-filling $\mu = 0$ and the Fermi surface is a perfect square. Using RPA we can calculate the spin-spin correlation function (see discussion in Chapter 12).

$$\begin{aligned} \chi_s(q,\omega) &= \frac{\chi_0(q,\omega)}{1 - U\chi_0(q,\omega)} \\ \chi_0(q,\omega) &= \int \frac{d^2k}{(2\pi)^2} \frac{n_{k+q} - n_k}{\omega - (\epsilon_{k+q} - \epsilon_k) + i0} \end{aligned} \tag{16.6}$$

At half-filling the Fermi surface has a nesting property. There exists nesting vector $Q = (\pi, \pi)$ which connects opposite sides of the Fermi sea (see fig. 16.3). When q approaches the nesting vector Q

$$\chi_0(\vec{q}, \omega = 0) \sim \nu(0) \log \frac{1}{|\vec{q} - \vec{Q}|} \tag{16.7}$$

Analogously there is divergence as we lower the temperature

$$\chi_0(\vec{Q}, \omega = 0, T) = \frac{1}{2\pi^2 t} \log^2 \left(\frac{16e^\gamma}{\pi} \frac{t}{T} \right) + \mathrm{C}_0 \tag{16.8}$$

where $C_0 \approx -0.0166$. These specific numbers are for for $d = 2$[26]. However analogous divergence exists in $d = 3$ as well. This means that for any finite $U > 0$ there is instability to the AF state. The normal state is unstable and the true ground state is the one with a static antiferromagnetic order. From equation (16.8) we find

$$T_N = \frac{16e^\gamma}{\pi} t \, exp \left(-\sqrt{2}\pi (\frac{t}{U} - C_0)^{1/2} \right) \tag{16.9}$$

To understand AF state we can do mean-field Hartree-Fock analysis with $\langle S^z_i \rangle = (-)^i N_0$. This corresponds to taking

$$U n_{i\uparrow} n_{i\downarrow} \to U \langle n_{i\uparrow} \rangle \, n_{i\downarrow} + U n_{i\uparrow} \, \langle n_{i\downarrow} \rangle - U \langle n_{i\uparrow} \rangle \langle n_{i\downarrow} \rangle \tag{16.10}$$

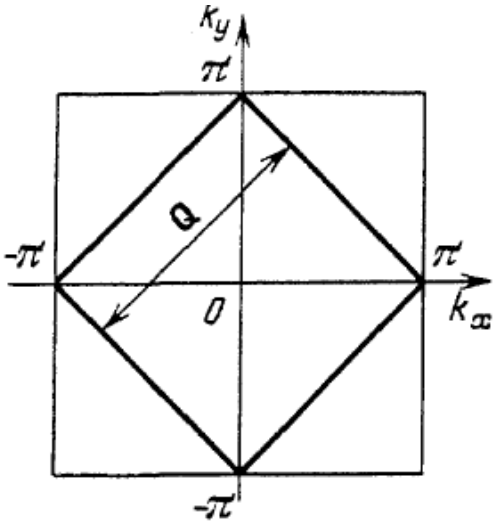

Figure 16.3: Brillouin zone for a square lattice. Diamond shows a Fermi surface at half-filling for non-interacting fermions. This Fermi surface has substantial parallel segments. This is the so-called nesting property.

Self-consistency equations for N_0 need to be solved.

16.2.3 Phase diagram at half-filling

By combining results of the two previous subsections we obtain a phase diagram in fig. 16.4. Note that while there is a maximum in the transition temperature, there is no maximum in the entropy at the transition point.

16.3 Away from half-filling

16.3.1 Attraction between holes

Motion of a hole in an antiferromagnetic background creates a string of flipped spins (see fig. 16.5). Thus we find effective attraction between holes. This suggests the possibility of pairing. To understand the character of pairing we consider a single plaquette as shown in fig. 16.6 [22]. For large U the largest real space amplitude in the four particle ground state are for the Neel configuration

$$\begin{aligned} |\Phi_a\rangle &= c^\dagger_{1\uparrow}\, c^\dagger_{2\downarrow}\, c^\dagger_{3\uparrow}\, c^\dagger_{4\downarrow}\, |0\rangle \\ |\Phi_b\rangle &= c^\dagger_{1\downarrow}\, c^\dagger_{2\uparrow}\, c^\dagger_{3\downarrow} c^\dagger_{4\uparrow}\, |0\rangle \end{aligned} \tag{16.11}$$

Now let us consider the ground state for two particles. When $U = 0$ we have

$$|\tilde{\Psi}_2\rangle = (c^\dagger_{1\uparrow} + c^\dagger_{2\uparrow} + c^\dagger_{3\uparrow} + c^\dagger_{4\uparrow})\,(c^\dagger_{1\downarrow} + c^\dagger_{2\downarrow} + c^\dagger_{3\downarrow} + c^\dagger_{4\downarrow})\,|0\rangle \tag{16.12}$$

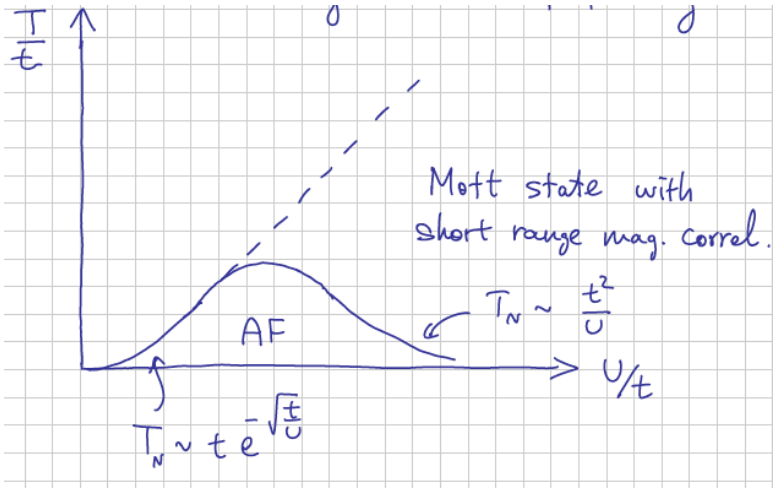

Figure 16.4: Phase diagram of the half-filled Hubbard model

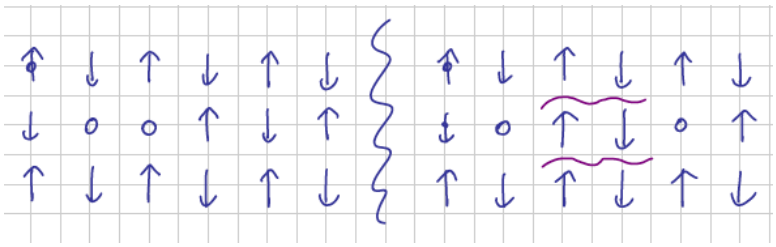

Figure 16.5: As holes separate they make a line of flipped spins. This increases the magnetic energy of the system. This "magnetic string" formation leads to an effective attraction between holes.

For large U we need to multiply $|\tilde{\Psi}_2\rangle$ by a projection operator that remives double occupancies

$$|\Psi_2\rangle = \left(c^\dagger_{1\uparrow} c^\dagger_{2\downarrow} + c^\dagger_{1\uparrow} c^\dagger_{3\downarrow} + \cdots \right) |0\rangle \tag{16.13}$$

We can now ask what is the operator that creates $|\Psi_2\rangle$ out of $|\Phi_a\rangle$ and $|\Phi_b\rangle$. We consider s and d-wave operaotrs defined in figures **??**. Simple calculation shows that

$$\begin{aligned} \langle \Psi_2 | \, \Delta_d \, | \Phi_{\{a,b\}} \rangle &\neq 0 \\ \langle \Psi_2 | \, \Delta_s \, | \Phi_{\{a,b\}} \rangle &= 0 \end{aligned} \tag{16.14}$$

This suggests that we should find d-wave pairing. One can define a pair-binding energy in one plaquette

$$\Delta_{\text{bind}} = 2E_g(N=3) - E_g(N=4) - E_g(N=2) \tag{16.15}$$

here $E_g(N)$ is the energy of the ground state in a plaquette with N fermions. Figure 16.9 shows pair binding energy as a function of U/t.

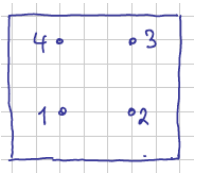

Figure 16.6: A four site plaquette

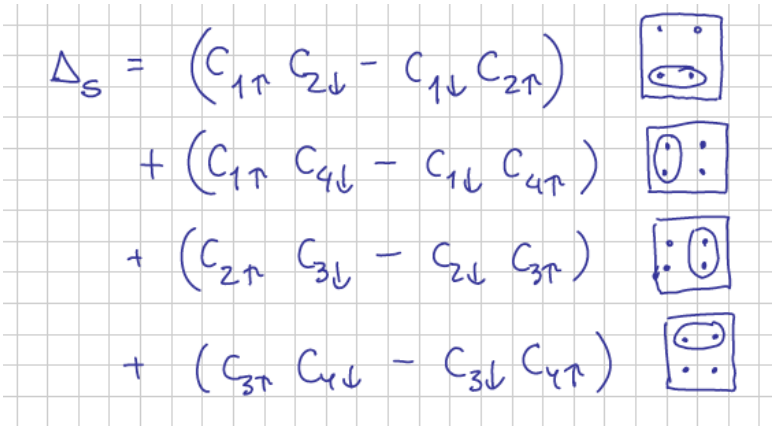

Figure 16.7: S-wave pairing operator defined on a plaquette

16.3.2 *d*-wave pairing mediated by paramagnon exchange

There is another way to think about pairing of holes in the background of strong magnetic fluctuations. Let us go back to conventional BCS mechanism superconductivity first. Phonon mediated pairing can be viewed the following way: Suppose we have an electron in a crystal of ions. This electron will attract positive ions and create a screening cloud of positive charges in the vicinity. After the electron moves on, the ions remain displaced from their original unpolarized state for some time due to their heavy mass. While the lattice is still partially polarized, a second electron can be attracted to the polarization cloud of ions and the energy of the system can be lowered. In this way an effective attraction is generated between electrons. Note that such interaction is retarded in time, which is important for the BCS theory. Retarded character of the lattice mediated attraction allows it to overcome the direct electron-electron repulsion[24].

A similar phenomenon can take place in an interacting electron system in the absence of phonons. The only difference is that in this case the polarization medium is not distinct from the electrons which are attracted. Consider the case of spin polarization. One electron produces a spin polarization cloud in the neighboring electron liquid. This spin polarization persists for some time before dying out. The second electron can interact with the spin polarization induced by the first electron and will be either attracted or repelled depending on its spin. In this way a spin dependent effective interaction is geerated. Just as one thinks of the lattice polarization mechanism as exchange of virtual phonons, one

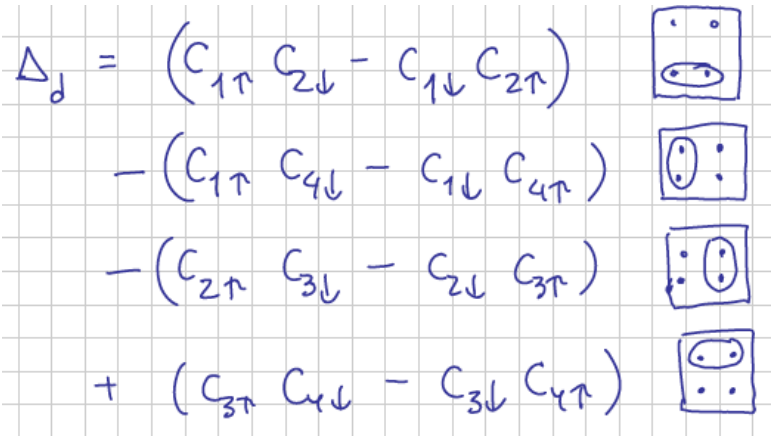

Figure 16.8: D-wave pairing operator defined on a plaquette

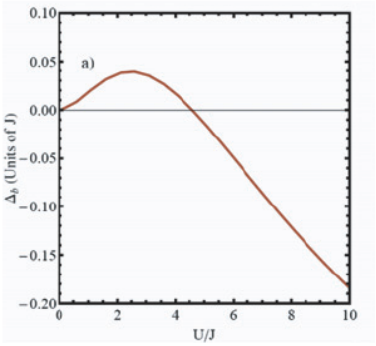

Figure 16.9: Pair-binding energy in a Hubbard plaquette[7]. When pair binding energy is positive it is energetically favorable to put holes into plaquettes in pairs.

may think of the process which we just described as equivalent to exchange of a virtual paramagnon.

In the phonon mechanism, the lattice constitutes essentially an independent system and its motion is affected very little by what is going on in the electron gas. Consequently, when the electron gas becomes superconducting, the response of the lattice is practically unaffected. In the case of the spin polarization mechanism, the medium, which is polarized, is the same as electrons undergoing the transition. Therefore, if as a result of attraction the behavior of electrons is changed (e.g. after they form Cooper pairs) the response of the polarization medium is automatically affected. Hence we need to consider feedback processes between spin fluctuations and pairing. One can use RPA type analysis to calculate BCS type coupling constants for different components of the order parameter (see fig. 16.10).

Another way to understand the origin of d-wave pairing is to consider the

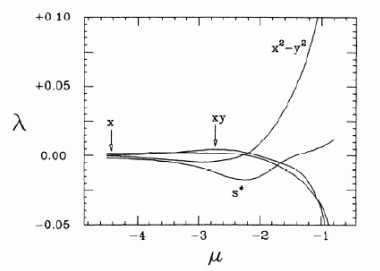

Figure 16.10: Effective BCS coupling constants for the Hubbard model computed using RPA type analysis. $d_{x^2-y^2}$ component strongly dominates near half-filling. It is defined as $\Delta_k = \cos k_x - \cos k_y$. Figure taken from [23].

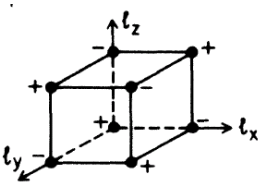

Figure 16.11: Real space picture of effective interaction for fermions mediated by magnetic fluctuations. Note that it changes sign depending on the distance and direction. Figure taken from [23].

BCS equation on the pairing amplitude.

$$\Delta_k = -\sum_{k'} V(k,k') \frac{\Delta_{k'}}{E_{k'}} \tag{16.16}$$

Within paramagnon exchange model we expect $V(k,k') \sim \chi(k-k')$. When the system is close to an AF instability and $k-k'$ is around Q, $\chi(Q)$ should be large and positive. Hence we expect $\Delta_{k+Q} = -\Delta_k$. This is satisfied for $\Delta_k = \cos k_x - \cos k_y$ (see fig. 16.12).

16.3.3 Alternatives to pairing

Another possibility is that holes make bound states of more than two particles. A state that often arises in mean-field calculations is a stripe phase shown in figure 16.13. Such states have been obtained in Hartree-Fock calculations [25, 29] and DMRG analysis of ladders[27]. Many neutron scattering experiments on high Tc cuprates have been interpreted in terms of stripe phases.

Other types of ordered phases have been considered away from half-filling, such as canted antiferromagnetic phase and spin spiral. However most of them appear to be unstable to phase separation.

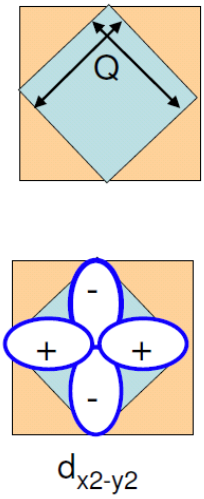

Figure 16.12: d-wave pairing arising from the AF magnetic fluctuations.

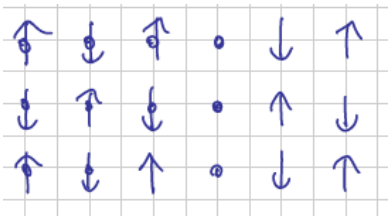

Figure 16.13: Schematic picture of a stripe phase

16.4 Current experiments with fermions in optical lattices

Current experiments reached the Mott insulating regime where double occupancies are strongly suppressed[12, 14]. Results of experiments demonstrating strongly interacting nature of the Hubbard mode and the appearance of incompressibility are shown in figs. 16.14 and 16.16. Recent experiments by T. Esslinger et al. [8] and R. Hulet et al. [11] demonstrated strong enhancement of antiferromagnetic correlations in the fermonic Hubbard model at low temperatures but no magnetic order yet. The lowest temperature achieved in experiments so far corresponds to 1.4 of the AF ordering temperature [11].

Interesting experiments have also been on done on exploring dynamics of fermions in a lattice. This includes probing fermions using lattice modulation experiments[12], measuring doublon lifetime[10, 13], and analyzing expansion of interacting particles[15].

It is also worth mentioning that for negative scattering length we find attractive Hubbard model which has been studied in detail using Monte Carlo[20]. It has been studied experimentally in [9].

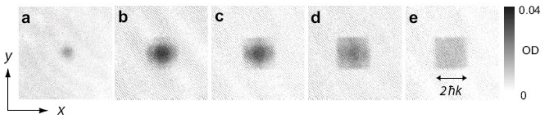

Figure 16.14: TOF experiments with nninteracting fermions in an optical lattice. At small densities the Fermi surface is nearly spherical. At larger fillings fermions fill up the entire Brillouin zone. Figure taken from [6].

Mixtures of fermions and bosons in optical lattices have also been studied in recent experiments[17, 21, 5].

16.5 Problems to Chapter 16

Problem 1.

A common model for discussing the high T_c cuprates is the t-J model with the Hamiltonian

$$\mathcal{H} \;=\; -t \sum_{<ij>} P_s \,\cdot\, C^+_{i\sigma}\, C_{j\sigma} \,\cdot\, P_s \;+\; J \sum_{<ij>} \vec{S}_i\, \vec{S}_j \;;\; J \;>\; 0.$$

Here $< ij >$ denotes the nearest neighbors and P_s projects out the states with two electrons on one site (so only states with 0 or 1 electrons per site exist in the Hilbert space of the t-J model). In this problem you will study the t-J model on a 4 site plaquette.

a) When there is exactly 4 electrons per 4 sites, the t-J model reduces to the AF Heisenberg model. Show that the ground state in this case is

$$|\psi_4> = \frac{1}{2}(S^+_{12}\, S^+_{34} \;-\; S^+_{14}\, S^+_{23})\, |vacuum>$$

where

$$\underline{S^+_{ij} \;=\; (C^+_{i\uparrow}\, C^+_{j\downarrow} \;-\; C^+_{i\downarrow}\, C^+_{j\uparrow})}$$
$$\sqrt{2}$$

Hint: Write the Heisenberg Hamiltonian as

$$J(\vec{S}_1\,\vec{S}_2 + \vec{S}_2\,\vec{S}_3 + \vec{S}_3\,\vec{S}_4 + \vec{S}_4\,\vec{S}_1) \;=\; \frac{J}{2}(\vec{S}_1 + \vec{S}_2 + \vec{S}_3 + \vec{S}_4)^2 - J(\vec{S}_1\,\vec{S}_3 + \vec{S}_2\,\vec{S}_4),$$

and construct a state for which $\vec{S}_{tot} = 0$, but $\vec{S}_1 \cdot \vec{S}_3$ and $\vec{S}_2 \cdot \vec{S}_4$ are maximized.

b) Find the ground state for two electrons $|\psi_2)$.

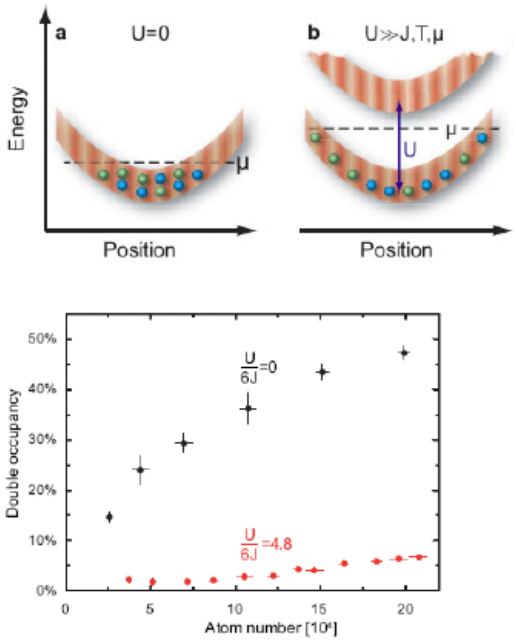

Figure 16.15: Measurements of doublon density as a probe of the Mott state. Figure taken from [12].

c) Take the definition of the $d_{x^2-y^2}$ Cooper pair creation operator, $\tilde{\Delta}_{d_{x^2-y^2}}$, as in the notes:

$$\tilde{\Delta}^{\dagger}_{d_{x^2-y^2}} = S^{\dagger}_{12} + S^{\dagger}_{43} - S^{\dagger}_{14} - S^{\dagger}_{23}$$

Compute $< \psi_4 \,|\, \tilde{\Delta}^{+}_{dx^2-y^2} \,|\, \psi_2 >$

d) Define the "extended s-wave" Cooper pair creation operator as

$$\tilde{\Delta}^{+}_{s^*} = (S^{+}_{12} + S^{+}_{43} + S^{+}_{14} + S^{+}_{23})$$

Compute $< \psi_4 \,|\, \tilde{\Delta}^{+}_{s^*} \,|\, \psi_2 >$

Problem 2

Consider fermionic alkaline-earth atoms with mass M and nuclear spin I trapped in an optical lattice. The internal state $|\alpha m\rangle$ of one such atom is specified by the electronic state α $(= g, e)$ and by the nuclear spin projection m,

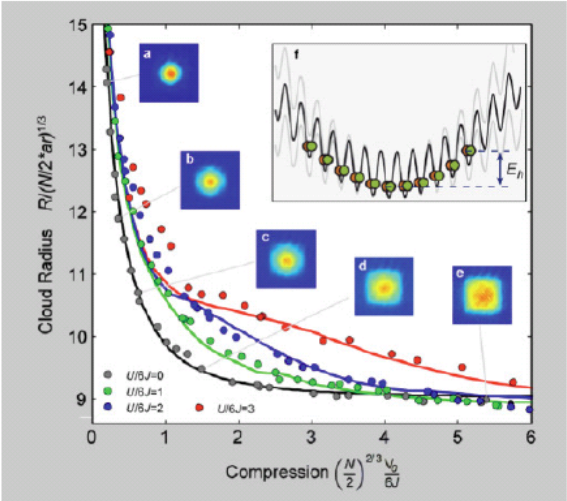

Figure 16.16: Measurements of the incompressible character of the Mott state. Figure taken from [14].

which runs over $N = 2I + 1$ nuclear Zeeman levels. In first-quantized notation, the Hamiltonian is

$$H = \sum_p H_p + \frac{1}{2}\sum_{p\neq q} H_{pq}, \tag{16.17}$$

where indices p, q run over the atoms. The one-body Hamiltonian is ($\hbar = 1$)

$$H_p = -\frac{1}{2M}\nabla_p^2 + \sum_\alpha |\alpha\rangle_p\langle\alpha|V_\alpha(\mathbf{r}_p), \tag{16.18}$$

where $V_\alpha(\mathbf{r}) = V_{0\alpha}[\sin^2(kx) + \sin^2(ky) + \sin^2(kz)]$ is the potential seen by electronic state α, and $|\alpha\rangle_p\langle\alpha|$ projects atom p on orbital state α. Pairwise s-wave interactions are

$$H_{pq} = \delta(\mathbf{r}_p - \mathbf{r}_q)\frac{4\pi}{M}(a_{gg}|gg\rangle\langle gg| + a_{ee}|ee\rangle\langle ee| + a_{eg}^+|eg\rangle_{++}\langle eg| + a_{eg}^-|eg\rangle_{--}\langle eg|). \tag{16.19}$$

Here $|eg\rangle_{\pm\pm}\langle eg|$ is the projection operator on $|eg\rangle_\pm$. $|\alpha\alpha\rangle = |\alpha\rangle_p|\alpha\rangle_q$ and $|eg\rangle_\pm = (|e\rangle_p|g\rangle_q \pm |g\rangle_p|e\rangle_q)/\sqrt{2}$. $a_{\alpha\alpha}$ and $a_{eg}^\pm$ are the four s-wave scattering lengths.

(a) Assuming that only the lowest band is occupied, derive the Hubbard Hamiltonian

$$\begin{aligned} H' &= -\sum_{\langle j,i\rangle\alpha,m} J_\alpha(c_{i\alpha m}^\dagger c_{j\alpha m} + c_{j\alpha m}^\dagger c_{i\alpha m}) + \sum_{j,\alpha}\frac{U_{\alpha\alpha}}{2}n_{j\alpha}(n_{j\alpha}-1) \\ &\quad + V\sum_j n_{je}n_{jg} + V_{ex}\sum_{j,m,m'} c_{jgm}^\dagger c_{jem'}^\dagger c_{jgm'}c_{jem} \end{aligned} \tag{16.20}$$

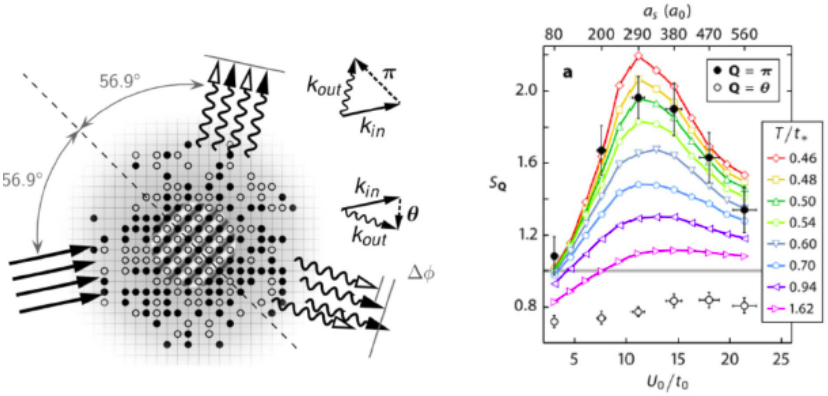

Figure 16.17: Measurements of spin correlations in the fermonic Hubbard model by R. Hulet et al. [11].

and express J_α, $U_{\alpha\alpha}$, V, and V_{ex} in terms of M, the four scattering lengths, $V_g(\mathbf{r})$, $V_e(\mathbf{r})$, and the Wannier functions $w_\alpha(\mathbf{r}-\mathbf{r_j})$, where $\mathbf{r_j}$ is the center of site j. Here $c^\dagger_{j\alpha m}$ creates an atom in internal state $|\alpha m\rangle$ at site j, $n_{j\alpha m} = c^\dagger_{j\alpha m} c_{j\alpha m}$, and $n_{j\alpha} = \sum_m n_{j\alpha m}$. The sum $\langle j, i\rangle$ is over pairs of nearest neighbor sites i, j. Constant terms, proportional to $\sum_j n_{j\alpha}$, are omitted in Eq. (16.20).

(b) Define SU(2) orbital algebra via

$$T^\mu = \frac{1}{2} \sum_{jm\alpha\beta} c^\dagger_{j\alpha m} \sigma^\mu_{\alpha\beta} c_{j\beta m}, \tag{16.21}$$

where σ^μ ($\mu = x, y, z$) are Pauli matrices in the $\{e, g\}$ basis. Verify that $[T^z, H'] = 0$. This U(1) symmetry follows from the elasticity of collisions as far as the electronic state is concerned.

(c) Define nuclear-spin permutation operators

$$S^m_n = \sum_{j,\alpha} c^\dagger_{j\alpha n} c_{j\alpha m}. \tag{16.22}$$

Verify that $[S^m_n, H'] = 0$ for all n, m. This SU(N) symmetry follows from the independence of scattering lengths and of the trapping potential from the nuclear spin.

(d) Derive the conditions on J_g, J_e, U_{gg}, U_{ee}, V, and V_{ex}, under which the U(1) orbital symmetry is enhanced up to a full SU(2) symmetry: $[T^z, H'] = [T^y, H'] = [T^z, H'] = 0$.

Bibliography

[1] editor A. Lebed. *The Physics of Organic Superconductors and Conductors*. Saunders College Publishers, 2002.

[2] P. W. Anderson. *Phys. Rev.*, 115:2, 1959.

[3] P. W. Anderson. *Science*, 235:1196, 1987.

[4] N. Ashcroft and N. Mermin. *Solid State Physics*. Saunders College Publishers, 2002.

[5] Th. Best, S. Will, U. Schneider, L. Hackermüller, D. van Oosten, I. Bloch, and D.-S. Lühmann. Role of interactions in $^{87}rb - ^{40}k$ bose-fermi mixtures in a 3d optical lattice. *Phys. Rev. Lett.*, 102(3):030408, Jan 2009.

[6] T. Esslinger. *arXiv:1007.0012*, 2010.

[7] A.M. Rey et al. *EPL*, 87:6001, 2009.

[8] J. Imriska et al. *Phys. Rev. Lett.*, 112:115301, 2013.

[9] L. Hackermueller et al. *Science*, 327:1621, 2009.

[10] N. Strohmaier et al. *Phys. Rev. Lett.*, 104:80401, 2010.

[11] R. Hart et al. *arXiv:1409.8348*, 2014.

[12] R. Joerdens et al. *Nature*, 450:268, 2008.

[13] R. Sensarma et al. *arXiv:1001.3881*, 2010.

[14] U. Schneider et al. *Science*, 322:1520, 2008.

[15] U. Schneider et al. *arXiv:1005.3545*, 2010.

[16] Z.Y. Meng et al. *Nature*, 464:847, 2010.

[17] Kenneth Günter, Thilo Stöferle, Henning Moritz, Michael Köhl, and Tilman Esslinger. Bose-fermi mixtures in a three-dimensional optical lattice. *Phys. Rev. Lett.*, 96(18):180402, May 2006.

[18] M. Imada H. MOrita, S. Watanabe. *JPSJ*, 71:2109, 2002.

[19] Masatoshi Imada, Atsushi Fujimori, and Yoshinori Tokura. Metal-insulator transitions. *Rev. Mod. Phys.*, 70(4):1039–1263, Oct 1998.

[20] R. Micnas, J. Ranninger, and S. Robaszkiewicz. Superconductivity in narrow-band systems with local nonretarded attractive interactions. *Rev. Mod. Phys.*, 62(1):113–171, Jan 1990.

[21] S. Ospelkaus, C. Ospelkaus, O. Wille, M. Succo, P. Ernst, K. Sengstock, and K. Bongs. Localization of bosonic atoms by fermionic impurities in a three-dimensional optical lattice. *Phys. Rev. Lett.*, 96(18):180403, May 2006.

[22] D. Scalapinio and S. Trugman. *arXiv:cond-mat/9604008*, 1996.

[23] D. J. Scalapino, E. Loh, and J. E. Hirsch. d-wave pairing near a spin-density-wave instability. *Phys. Rev. B*, 34(11):8190–8192, Dec 1986.

[24] J.R. Schrieffer. *Theory of Superconductivity.* Addison-Wesley Publishing Company, 1983.

[25] H. J. Schulz. Incommensurate antiferromagnetism in the two-dimensional hubbard model. *Phys. Rev. Lett.*, 64(12):1445–1448, Mar 1990.

[26] Shimahara and Takada. *JPSJ*, 57:1044, 1988.

[27] Steven R. White and D. J. Scalapino. Phase separation and stripe formation in the two-dimensional $t - j$ model: A comparison of numerical results. *Phys. Rev. B*, 61(9):6320–6326, Mar 2000.

[28] J. Zaanen, G. A. Sawatzky, and J. W. Allen. Band gaps and electronic structure of transition-metal compounds. *Phys. Rev. Lett.*, 55(4):418–421, Jul 1985.

[29] Jan Zaanen and Olle Gunnarsson. Charged magnetic domain lines and the magnetism of high-t_c oxides. *Phys. Rev. B*, 40(10):7391–7394, Oct 1989.